Quaternary Science Reviews 293 (2022) 107719

Contents lists available at ScienceDirect

Quaternary Science Reviews

journal homepage: www.elsevier.com/locate/quascirev

Sea-level change, palaeotidal modelling and hominin dispersals: The case of the southern red sea

Jon Hill [a, *], Alexandros Avdis [b], Geoff Bailey [c, d], Kurt Lambeck [e]

[a] Department of Environment and Geography, University of York, UK
[b] Department of Earth Science and Engineering, Imperial College London, UK
[c] Department of Archaeology, University of York, UK
[d] College of Humanities and Social Sciences, Flinders University, Australia
[e] Research School of Earth Sciences, Australian National University, Australia

ARTICLE INFO

Article history:
Received 25 May 2022
Received in revised form
11 August 2022
Accepted 11 August 2022
Available online xxx

Handling Editor: Dr Giovanni Zanchetta

Keywords:
Sea-level change
Shoreline reconstruction
Tidal modelling
Simulation
Hominin dispersal

ABSTRACT

We examine the likelihood of early human sea crossings of the southern Red Sea during Pleistocene low sea-level stands, using palaeotopographic reconstruction of coastlines, modelling of palaeo-tidal flows and simulation of passive movements using Lagrangian particles. Existing isotopic and geological data demonstrate that the marine connection between the Red Sea and the Indian Ocean has remained open for at least the past half million years, ruling out the possibility of a land crossing. Many authors have argued for the plausibility of a successful sea crossing during the Pleistocene as a southern route for human dispersal from Africa, especially for the dispersal of *Homo sapiens*. However, decisive evidence is lacking. Other authors have preferred the default northern route of land-based dispersal via the Sinai Peninsula as the more likely option and viewed the southern sea crossing as a barrier rather than a gateway, especially if tidal flow was much stronger through the narrowed sea channel at low sea levels. We use Fluidity, a finite element modelling procedure, to model tidal flows and assess their validity by comparison with modern tide-gauge data. To model palaeotidal flows, we use reconstructions of palaeoshorelines and coastal palaeotopography extending for 150 km from the Bab al Mandab Strait to the Hanish Sill region, which take account of eustatic, GIA and tectonic effects. We then simulate passive movements using Lagrangian particles and a 4th-order guided search Runge-Katta algorithm. We ran simulations for six days from three different starting points on the African shore and 13 different times in the tidal cycle. We show that crossing distances are much shorter during the Pleistocene than today with clear inter-visibility of the opposing shorelines, but that tidal currents were much stronger. We also show that the highest chances of successful crossing, involving passive rafting or drifting, with a duration of 3–4 days, are in the vicinity of the islands in the Hanish sill region. With directed rafting or swimming, the crossing times would be much shorter. We conclude that sea crossings would be easily accomplished during long periods of the glacial cycle, regardless of hominin status, especially given attractive terrestrial landscapes and environments on both sides of the southern Red Sea.

1. Introduction

According to a widely held consensus, Africa is the centre of origin of the earliest developments in the human evolutionary trajectory, and human colonisation of other parts of the world was the result of population dispersal out of Africa beginning at about 2 million years ago (Joordens et al., 2013). The number of pulses of dispersal out of Africa, the hominin species involved, and the most likely pathways and directions of movement are matters of ongoing debate. At least two waves of dispersal are currently recognised, an earlier one at or soon after 2 Mya by earliest members of the genus Homo, and a later one by *H. sapiens* that took place, according to genomic data, about 70,000 years ago if not earlier (Abbate and Sagri, 2012; Bolus, 2015; Dennell, 2008; Groucutt et al., 2015; Lahr and Foley, 1994a; López et al., 2015; Martínez-Navarro, 2010).

The most obvious terrestrial pathway out of Africa from late Pliocene – early Pleistocene times onwards is the relatively narrow corridor of land at the northern end of the Red Sea connecting the

* Corresponding author.
E-mail address: jon.hill@york.ac.uk (J. Hill).

https://doi.org/10.1016/j.quascirev.2022.107719

mouth of the River Nile via the Sinai Peninsula to the southern Levant, which has generally been assumed to have been the default option for large terrestrial mammals and early hominins. At its narrowest, this coastal corridor is a ~50-km-wide semi-arid coastal plain backed by the foothills and mountains of the Sinai Peninsula. It would have become wider and potentially more attractive periodically during the Pleistocene, resulting from extension of the Mediterranean coastline and infilling of the Gulf of Suez during periods of low sea level (Bailey et al., 2007, 2008; Lambeck, 2004) and from climatic and vegetational change associated with periodic 'greening' of the Sahara and Arabian deserts (Larrasoaña et al., 2013; Petraglia et al., 2019; Rohling et al., 2013). This would have opened up easier pathways of movement to the east and south into the Arabian Peninsula as well as northwards to the Levant and Anatolia. Nevertheless, it would have remained at all periods a topographic and environmental bottleneck in the larger geographical setting and one vulnerable to palaeoclimatic oscillations.

Sea crossings have long been recognised as alternative pathways of movement both across some of the narrower sea channels of the Mediterranean and at the southern end of the Red Sea (Fig. 1), and recent investigations have intensified an interest in these possibilities (Alimen, 1975; Bednarik, 1999; Beyin, 2006; Gaffney, 2021; Hölzchen et al., 2022; Runnels, 2014; Straus, 2001). Moreover, evidence from island SE Asia that rafting across a distance of at least 19 km presumably by *Homo erectus* to the island of Flores took place ~1 million years ago (Brumm et al., 2010; Dennell et al., 2014) and that Sahul (Australia and New Guinea) were colonised by sea by at least 50 ka across distances of 50 km or more by anatomically modern humans, *Homo sapiens* (AMH) (Clarkson et al., 2017; Allen and O'Connell, 2008; Bird et al., 2018) has reinforced an expectation that similar evidence at earlier dates should be found in other parts of the world.

The issue of viable pathways out of Africa is of particular importance to an understanding of hominin dispersals because the existence of alternative routes as viable pathways of movement opens up multiple possibilities for the timings and patterns of dispersal and species interaction and evolution. However, investigation of these possibilities in Africa and Eurasia has been hampered: by ambiguities in the available evidence; by preconceptions as to whether sea channels constituted a barrier to movement or a gateway; by assumptions about the technological and cognitive capacity of earlier hominin populations to undertake sea crossings; by uncertainties about the likely mode of sea travel – whether by accidental drifting (sweepstake movements), swimming, rafting, directional movement, construction of boats with oars or sails, and use of navigational skills; and above all by absence of or incomplete information of past coastlines. Hölzchen et al. (2022) have recently modelled potential sea crossings in the Mediterranean and the Red Sea, with particular reference to such factors as human physiology, demography, movement and perception, using low-resolution environmental variables extrapolated from modern conditions. Here we use a different modelling approach to provide a detailed assessment of the palaeotopography and tidal currents of the southern Red Sea during a low sea-level stand. In the terminology of Hölzchen et al. (2022) we are simulating either passive drifting or passive rafting, but not accounting for any physiological properties.

1.1. Issues in palaeocoastal and palaeo-oceanographic reconstruction

A major variable that can have large effects on the interpretation of sea crossings is changes in the configuration of coastlines, land bridges, offshore islands, sea distances and ocean currents. Eustatic sea-level change in conjunction with modern bathymetry is well recognised as a first order approximation of coastal change. However, the pattern can be complicated at both the regional and the local scale by uplift and subsidence associated with glacio-hydro-isostatic crustal deformation in response to loading and

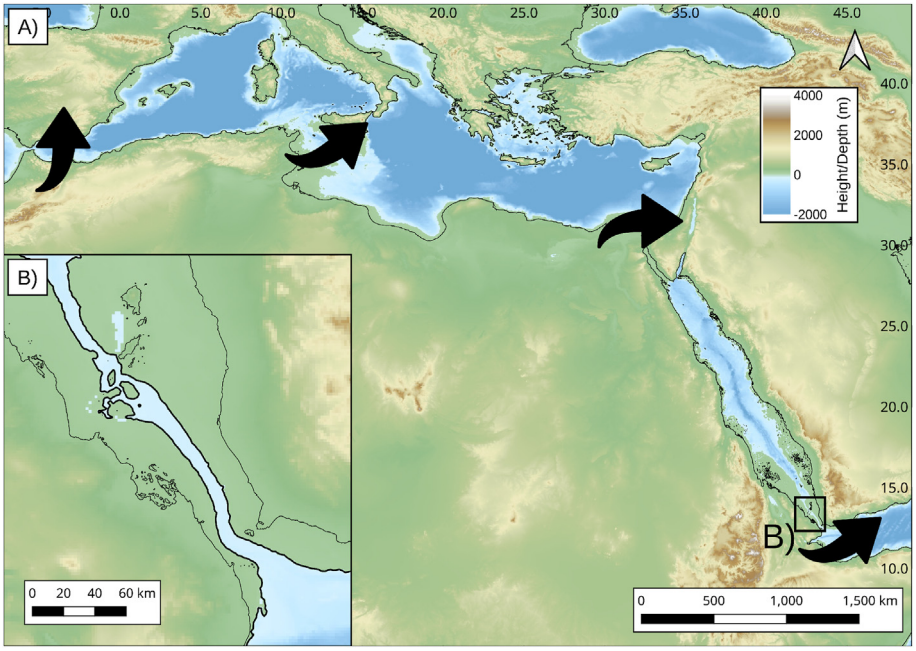

Fig. 1. Reconstruction of southern Europe, northern Africa and the Arabian peninsula at around 21 ka based on a modified sea-level construction of Lambeck et al. (2014) A). The thin line show modern coastlines. The two proposed routes to the Arabian peninsula are show with thick black arrows, along with routes into Europe across the Gibraltar Straits and via Italy. The southern crossing route of the palaeo-Red Sea is highlighted in B), where thin black indicate the modern coastline and thick black lines indicate the palaeo-coastline. (For interpretation of the references to colour in this figure legend, the reader is referred to the Web version of this article.)

unloading of continental ice sheets, of water masses, and of sediment loads on the seabed, and by tectonic activity associated with plate motions (Borreggine et al., 2022; Lambeck et al., 2004). All these processes are widely in evidence in the Mediterranean and some can have major effects on the reconstruction of coastlines, especially in the Aegean and as one goes further back in time in the Pleistocene (Antonioli et al., 2017; Canals et al., 2017; Chiocci et al., 2017; Lambeck, 1995, 1996; Lykousis, 2009; Sakellariou et al., 2017; Sakellariou and Galanidou, 2017).

Their potential significance is occasionally recognised in debates about early sea travel but more rarely acted on (but see Bird et al. (2018) for a recent example from Australia), while investigation of the drowned landscapes on the continental shelf where much of the relevant palaeoenvironmental and archaeological evidence must be sought is still in its infancy (Bailey, 2013, 2015; Flemming et al., 2017).

Localised geophysical analysis undertaken in relation to specific archaeological questions demonstrates that the potential for sea crossings is not simply a matter of reconstructing palaeoshorelines and sea distances, but also of ocean currents and tidal movements, especially in narrow channels, where the funnelling of marine currents produces highly variable conditions including extremes that can act as an effective deterrent to successful sea crossings, even over short distances. Ferentinos et al. (2012), for example, demonstrate that a channel 5–12 km wide remained open between the Greek mainland and the Ionian islands of Kephallinia and Zakynthos throughout the Pleistocene and was successfully crossed, apparently as early as the Middle Palaeolithic period (accepting the typological dating of the surface assemblages of stone tools). Conversely, the 2–3 km wide Messinian Strait between Sicily and Italy, famous in Classical mythology as a sailor's graveyard, was not successfully crossed until the formation of a narrow land bridge after ~26 ka at the Last Glacial Maximum (LGM), at which time Upper Palaeolithic stone industries and mainland fauna appear on Sicily, a relatively late occurrence attributed to difficulties of sea crossings because of the high speed of tidal currents in the Strait (Antonioli et al., 2016). Similarly, there is no evidence for the crossing of the 12 km-strait between the Italian mainland and the island of Corsica until the Mesolithic period, nor the 10 km channel between the island of Pianosa and the mainland until the Neolithic (Castagnino Berlinghieri et al., 2020). These are relatively short distances compared to the evidence of sea crossings to Australia or the claims for longer sea journeys across the Mediterranean during the Pleistocene (Broodbank, 2014; Ferentinos et al., 2012; Galanidou, 2014; Howitt-Marshall and Runnels, 2016; Kaczanowska and Kozłowski, 2014; Leppard, 2014b,a; Leppard and Runnels, 2017; Phoca-Cosmetatou and Rabett, 2014; Runnels, 2014). The point here is that short distances by themselves are no guarantee of successful sea crossings, and that other variables need to be considered, especially the configuration of coastlines and oceanic conditions as they would have existed when relative sea levels were lower than the present. Recent work has examined the impact of oceanic conditions and tides on the crossing to Sahul (Kiki Kuijjer et al., 2022; Bird et al., 2018) using similar methods to those used here.

1.2. The Red Sea

The southern crossing of the Red Sea has attracted wide attention as a potential exit from Africa (Bailey, 2010; Beyin, 2006, 2011; Lahr and Foley, 1994b; Oppenheimer, 2012; Petraglia and Alsharekh, 2003; Walter et al., 2000). The narrowest crossing at the present sea level is 29 km at the present day Bab al Mandab Strait, at the southern most point of the Red Sea. Cultural similarities between the Horn of Africa and southwest Arabia in the Neolithic period from ~8 ka onwards suggest the possibility, if not a definitive demonstration, of sea crossings; and boats made from bundles of reeds and bitumen were certainly in use in the Persian Gulf by this time (Carter, 2010; Durrani, 2005). How far back in time these capabilities can be extended remains uncertain. But, in any case the southern mouth of the Red Sea would have formed a long channel much narrower than at present at the LGM, extending for 150 km from the present-day Bab al Mandab northwards to the Hanish Sill region, with the shortest crossing points, ~5 km, via the mid-channel islands at the Hanish Sill (Fig. 1; Lambeck et al., 2011).

The seabed at the Hanish Sill is 137 m below present sea level, which is close to the maximum lowering of sea level during glacial maxima. However, isotopic data from deep-sea marine-sediment cores demonstrating continued exchange of seawater between the Red Sea and the Indian Ocean and modelling of palaeocoastlines incorporating isostatic and tectonic movements demonstrate that the marine channel has remained continuously open for at least the past 500 kyr (Grant et al., 2014; Lambeck et al., 2011; Rohling et al., 2013). Reconstruction before 500 ka is less certain, due to lack of older marine-sediment cores and a more limited record of palaeoshoreline deposits with which to calibrate the global eustatic sea-level curve against earth movements. However, geological, geophysical and neotectonic data indicate that formation of evaporites (salt deposits) associated with a closed basin ceased at the end of the Miocene ~5 million years ago, implying a continuous marine connection with the Indian Ocean since then. This then implies that the geometry of the channel has remained largely unchanged despite progressive opening of the Red Sea, with deformation resulting from the separation of the Arabian and African plates accommodated in adjacent regions such as the Afar rather than the immediate vicinity of the channel itself (Augustin et al., 2019; Bosworth et al., 2019; Inglis et al., 2019a).

Other arguments in favour of this southern crossing are that it affords a direct route to southern Asia that bypasses the Sinai bottleneck and therefore offers an alternative pathway that better explains the apparent divergence in human evolutionary and cultural trajectories between Europe and SE Asia, especially with respect to AMH (Lahr and Foley, 1994a; Mellars, 2006). More recent versions of this hypothesis have combined phylogenetic interpretations of mtDNA in modern human populations with apparent increased evidence for exploitation of marine foods in the late Pleistocene, and seaborne entry into Sahul, to propose a rapid dispersal of AMH populations around the rim of the Indian Ocean from South Africa to Australia at about 70 or 60 ka, fuelled by new adaptations in seafaring and exploitation of marine resources developed by cognitively and technologically superior AMH populations (Macaulay et al., 2005; Mellars, 2006; Mellars et al., 2013). Many elements of this model have been challenged, especially the tight coupling of AMH dispersal, dependence on marine resources, seafaring, and coast-hugging pathways of dispersal throughout the 7000 km range of AMH expansion around the Indian Ocean rim. More regionally focused studies of similarities and differences in stone tool assemblages in NE Africa, Arabia and the Levant, and the distribution of genetic haplotypes, while suggestive, remain ambiguous especially regarding specific geographical centres of origin and pathways of dispersal (Bailey, 2015; Beyin, 2011; Boivin et al., 2013; Groucutt et al., 2015).

New field investigations in Saudi Arabia directed to resolving some of these ambiguities have crystallised around two alternative models of movements into and through Arabia. The ‘palaeodesert’ model emphasises the ‘Northern’ route with opening up of the Sinai region and the interior of the Arabian Peninsula during wetter climatic intervals in the Pleistocene. This wetter interval generated an expansion of grasslands, with streams and lakes, into desert regions, followed by the widespread dispersal of human and large-

mammal populations throughout the Arabian Peninsula attested by numerous archaeological sites including stone tools, fauna and human traces (Groucutt et al., 2015, 2018; Petraglia et al., 2019).

The alternative model, or southern route, emphasises the close proximity of attractive terrestrial environments on both sides of the southern Red Sea with relatively humid climate and a complex topography of fault-bounded basins and volcanic lavas. These conditions were conducive to trapping of sediments and water, ambush hunting of large mammals, and provision of stone raw materials. The expansion of similar conditions at lowered sea level onto an extensive and now-submerged territory in the southern Red Sea would mean improved groundwater supplies and a narrow sea crossing for long periods of the glacial cycle (Bailey, 2015; Bailey et al., 2015; Hausmann et al., 2021; Inglis et al., 2019b; Kübler et al., 2015; Lambeck et al., 2011; Sakellariou et al., 2019; Winder et al., 2015). Marine resources, especially molluscs, likely persisted at the southern end of the Red Sea throughout the glacial-interglacial cycle as an added incentive to visit the shoreline (Hausmann et al., 2021; Walter et al., 2000; Sergiou et al., 2022).

These two models are not necessarily incompatible, and both may have been significant, with greater emphasis on the interior during interglacial or interstadial episodes of the glacial-interglacial cycle, and on the coast and its immediate hinterland during periods of low sea level, a variation supported by more detailed analysis of climatic records (Rohling et al., 2013). Nevertheless, there is a difference of emphasis with respect to the use of coastal regions and sea crossings. The palaeodesert model prefers terrestrial pathways of dispersal along networks of rivers, stream channels and lakes on a broadly west to east axis, discounting coastal environments, marine resources and submerged landscapes. This model also points to the absence or rarity of coastal sites with evidence of marine resources around the coastlines of the Arabian Peninsula before the Holocene. This model therefore treats the persistence of the sea crossing in the south as a barrier rather than a gateway. The Southern coastal dispersal model, in contrast, emphasises the distribution of climatically insensitive landscapes (*sensu* King and Bailey, 1985; Bailey et al., 1993, 2011) on both sides of the southern Red Sea, the availability of fertile marine environments around the southern coastlines of the Arabian Peninsula as an added source of food, the significance of submerged landscapes, the abandonment of the desert interior for long periods of the climatic cycle, and the impact of sea-level change on the visibility or survival of coastal sites. Critical to both models are conditions in the Bab al Mandab – Hanish Sill channel and the relative ease or difficulty of making the water crossing.

1.3. Red sea tides and palaeotidal modelling

The Bab al Mandab – Hanish Sill channel is a key location for transfer of water from the Gulf of Aden to the Red Sea. The modern day channel is over 150 km long and is shallow compared to the Red Sea and Gulf of Aden basins to the north and south respectively. The overall flow along the channel is characterised by high salinity flow from the Red Sea (where evaporation is greater than precipitation) into the Gulf of Aden (Sofianos et al., 2002). Whilst this is a relatively small flow (0.36 Sv) it has a spatially large signal in the Indian Ocean (Murray and Johns, 1997). Flow through the straits is dominated by both low frequency ocean currents and higher frequency tidal motions, where the structure can be split into summer (June to September) and winter (October to May) flows. The summer flow is a three-layer system with shallow outflow of the Red Sea, and intermediate cold, fresh flow into the Red Sea and a deeper hypersaline flow out of the Red Sea. In winter, this is replaced by a two-layer system with hypersaline flow in the deeper layers from the Red Sea and relatively less saline water inflowing into the Red Sea at the surface (Murray and Johns, 1997). Peak velocities (including tidal flow, wind circulation and ocean circulation) were measured at around 1 m/s during summer 2001, in a series of anticyclone patterns (Sofianos et al., 2002).

In addition to the general ocean circulation described above, the barotropic tides in the area are relatively straightforward. The tides in the Red Sea are general semi-diurnal in character, but this can be irregular and in some places diurnal (Guo et al., 2018). Tides are largely dominated by the M_2 tidal constituent (a semi-diurnal lunar tidal component), but with a significant contribution from the K_1 tidal constituent (a diurnal lunar tidal component) also. Due to the lack of consistent data recording from tidal gauges around the Red Sea, modelling offers a method of understanding the tidal wave propagation in the Red Sea. Previous modelling studies (Madah et al., 2015; Guo et al., 2018) show good agreement to the limited data available and found that the semi-diurnal tides play a major role in the spatial distribution of the tidal range, except in the centre of the Red Sea. However, another study found that whilst the semi-diurnal tides were crucial, they were also harder to simulate accurately (Jarosz et al., 2005). The tidal range varies from 1 m at the Hanish Sill in the northern part of the channel to 2 m at the southern boundary. Typical tidal currents in the Bab al Mandab strait, where currents were highest, were found to be between 0.5 m/s (Madah et al., 2015) or 1 m/s (Jarosz et al., 2005) during flood conditions. In addition, Jarosz et al. (2005) found only weak residual currents up to 12 cm/s, focused particularly around the Hanish Islands. This indicates tides have a minimal role in the overall transport of water in and out of the Red Sea, but the fastest tides are significant in terms of instantaneous ocean transport.

However, since the LGM, sea levels have risen, as described above, changing the characteristics of the flow through the channel. Previous work has demonstrated the utility of palaeotidal modelling in quantifying the changes to tidal hydrodynamics caused by changes in sea level and coastal geomorphology (e.g. Collins et al., 2018; Davies et al., 2020; Wilmes and Green, 2014; Haigh et al., 2020). Previous work has focused on the European continental shelf in particular (e.g. Hinton, 1995; Austin, 1991) with later work incorporating Glacial Isostatic Adjustment (GIA) models to create palaeobathymetry (e.g. Scourse et al., 2009; Egbert et al., 2004; Uehara et al., 2006), which take into account spatial variation of the relative sea-level changes. Similar methods have been used to simulate geologically ancient palaeotides (e.g. Mitchell et al., 2010; Wells et al., 2007; Collins et al., 2017). Palaeotidal modelling can therefore give valuable insights into the changes of tidal dynamics in ancient landscapes.

Here, we assess the possibilities for early human movement during the Pleistocene across the southern end of the Red Sea, focusing in particular on a reconstruction of water currents and palaeotidal movements through the relatively narrow channel that developed during low stands along the section to the north and south of the Hanish Sill. We first describe the palaeotopographic reconstruction, then detail the tidal modelling, validating the model using modern data. Using the validated model we then simulate the palaeotidal flow, simulating rafting behaviour using passive tracer particles to assess the probability that these particles complete a journey across the Red Sea. We use these results to assess the viability of sea crossings for early hominin movements between Africa and Arabia during sea-level minima.

2. Methods and materials

2.1. Palaeotopographic/bathymetry reconstruction

The Red Sea bathymetric data used is the GEBCO-08 3" (900 m) grid dataset (the GEBCO-08 Grid, version 20090202, http://www.gebco.net) supplemented in the northern Bab al Mandab with higher resolution PERSGA data (Programme for the Environment of the Red Sea and Gulf of Aden; Gardline Surveys contractor) held by the UK Hydrographic Office. The area covers all shoals and channels south of Hanish with depth accuracies, corrected for sound velocity and tides, of the order 0.5–1.0 m and an average profile spacing of 108 m (see Lambeck et al., 2011, appendix). The principal feature is a continuous channel cutting across a broad topographic high with a sill, the Hanish Sill, ~25 km west of Hanish Island at 42.5°N, 13.75°E, Yemen, extending over ~5 km and at the same location as originally found by Werner and Lange (1975), such that if sea levels in the Gulf of Aden were to drop below ~205 m the Red Sea would become isolated.

Past bathymetry corresponds to present sea level less any sea-level change that occurred in the intervening period, changes resulting from sea-floor erosion or sedimentation, from tectonic land movements, and from changes in ocean volume and water distribution within the oceans. In the sill area itself, the topography appears to be smooth with a number of deeps and highs within the major channel (Lambeck et al., 2011). This along with current velocity measurements suggests that neither sedimentation nor bedrock erosion has been a major issue here (Mitchell and Sofianos, 2019). Despite a complex thermal-tectonic history of the Red Sea and Gulf of Aden, with volcanism into Holocene time (Boone et al., 2021; Bosworth et al., 2019; Smithsonian Institution, 2013), the African coast of the central and southern parts down to northern Djibouti appears to have been relatively stable since some time after the penultimate interglacial and before the Last Interglacial (e.g. Plaziat et al., 1998). A more pervasive and systematic cause of sea-level change on the millennial time scale is the cyclic growth and decay of the ice sheets that contribute both to a changing ocean volume and to concomitant land deformation in response to the changing ice-water loads. These are the GIA effects, for which the geophysical modelling is well established (Cathles, 1975; Farrell and Clark, 1976; Peltier, 1998; Mitrovica and Milne, 2003). The formulation used here is that of Nakada and Lambeck (1987); Johnston (1993) and Lambeck et al. (2003). One consequence is that the sea-level change becomes spatially variable and cannot be described by a single number such as eustatic sea level. Variations within the Red Sea during the LGM, for example, can be expected to range between ~-105 m in the northern Red Sea to ~-130 m m in the central part and ~-115 m at the Hanish Sill, compared with a globally averaged change of ~-135 m (Lambeck et al., 2011). The quantification of model parameters that define the response to the ice-load history are usually partially constrained by the sea-level observations themselves from areas free of vertical tectonic movements or for which the tectonic rates can be independently established. In addition, it is possible to achieve some separation of tectonic, isostatic and eustatic contributions through an iterative analysis of the sea level and glacial history evidence. Results for the Red Sea have been discussed in Lambeck et al. (2011) and used here, with minor updates from subsequent ice- and earth-parameters (Lambeck et al., 2014, 2017).

At the LGM the southern Red Sea was reduced to a narrow channel < 10 km wide at the Hanish sill location and bifurcated into narrower channels further south (Fig. 2). Profile B corresponds to a path between Africa and Arabia that involves a minimum water crossing of ~3 km by island-hopping via the now emerged shoals. Of some note is that because of the deep incision of the channel this configuration initially changes only slowly as global sea levels rise. Only by about 12 ka, when global sea levels were about 60 m below present, do channel widths expand, rapidly reaching ~25 km. In the

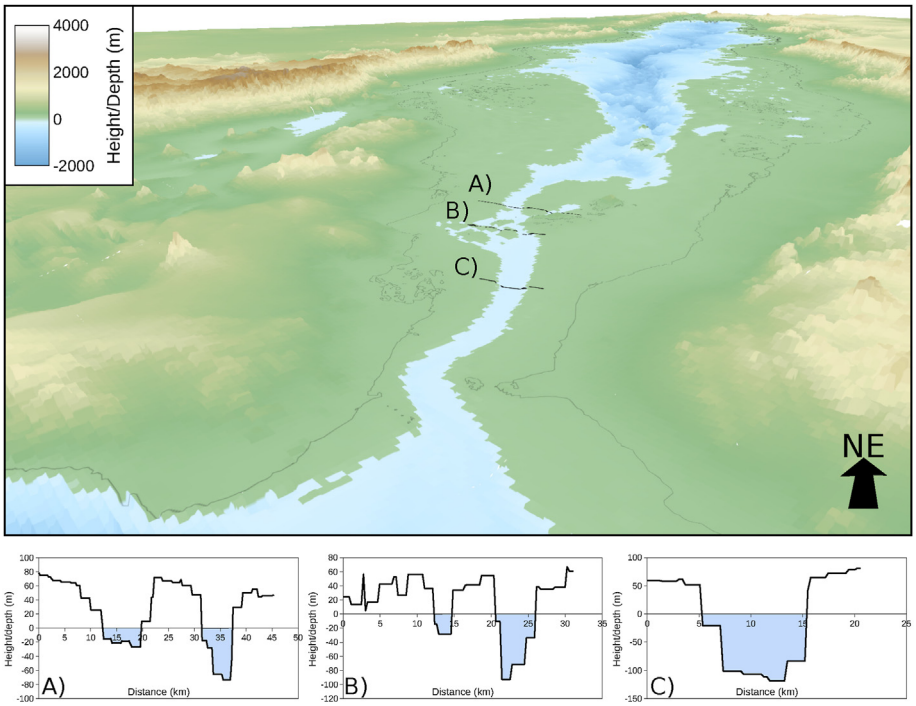

Fig. 2. 3D view of the reconstructed palaeo-topography across the Red Sea area at glacial sea-level minima. The black lines show three potential crossing points, with the height/depth shown in the cross sections below. The shortest distance to cross is ~3 km, via the mid-channel islands at the Hanish Sill - cross section B. (For interpretation of the references to colour in this figure legend, the reader is referred to the Web version of this article.)

pre-LGM period global sea levels were below ~50 m for lengthy periods such that these channel configurations with favourable crossing widths would not have been ephemeral but would have existed over intervals of several tens of thousands of years. At no time in the period relevant to AMH expansion out of Africa was there a dry land bridge across the southern Red Sea, but the channel is narrow enough to consider the possibility of crossings by simple swimming or rafting. The elevated banks during these low-stand periods would result in obvious inter-visibility between opposing shores and channels that would have persisted as narrow crossings for at least 40,000 years in a 100,000-year glacial cycle (Fig. 2 and supplementary information). Even the widest crossing (site 3, Fig. 2C) would have clear inter-visibility across the 10 km channel with sea-levels up to 40 m higher than at the LGM, and therefore the opposing shore would be visible for the entire duration of the crossing.

Extending these reconstructions further back in time becomes less certain, in part because the earlier ice history is less well known, although the limited information available for the penultimate glacial maximum sea levels (Spratt and Lisiecki, 2016) indicates that global sea level and ice volumes were similar to those for the LGM. Also, the occurrence of the Last Interglacial shorelines at about their 'expected' elevations suggests that tectonic contributions have been secondary such that the Hanish sill results for the LGM should also be indicative of conditions for the earlier maximum sea-level lowstand at ~140 ka. Our results and conclusions in general will therefore be applicable to those previous sea-level lowstands (Lambeck et al., 2011).

2.2. Tidal modelling

To simulate the tides in the Red Sea we use Fluidity, a highly flexible finite element/control volume modelling framework which allows for the numerical solution of a number of equation sets (Piggott et al., 2008) and has been used in a variety of flow studies ranging from laboratory-to ocean-scale (e.g. Hill et al., 2012, 2014; Parkinson et al., 2014; Smith et al., 2016). In a tidal modelling context, Fluidity has been used to model both modern and ancient tides on regional and global scales (e.g. Mitchell et al., 2010; Wells et al., 2010; Collins et al., 2018, 2017; Martin-Short et al., 2015). Full details of the model equations and discretisation are given in the supplementary information.

2.2.1. Model setup

Fig. 3 shows the geometry of the model used in this study. The domain boundaries are composed of contours representative of shorelines and open boundaries. The domain boundaries were assembled using QGIS (QGIS Development Team, 2016) and the meshes were generated using qmesh (Avdis et al., 2018). At the shorelines the modelling approach does not attempt to capture shoaling effects, nor the periodic exposure and submergence of low-lying areas due to tidal inundation. In large-scale models simulating such effects is impractical, so the minimum depth was set to 3 m to ensure simulations did not require computationally expensive wetting-and-drying algorithms. Coastlines were either derived from GSHHS data (Wessel and Smith, 1996) or the 0 m contour of the reconstructed bathymetry. The application of the code requires a number of model parameters and other decisions that ensure numerical stability of the solutions as well as physically realistic outcomes. These choices are based on various tidal modelling tests for different regions with different configurations and representative results have been adopted here (Martin-Short et al., 2015; Mitchell et al., 2010; Collins et al., 2017, 2018). The most pertinent parameter that affects the tidal flow and has greatest uncertainty is the drag coefficient. We have set this to a value equivalent to clean sand bed (see below) to minimise any assumptions on bed type both in the modern and palaeo simulations. As part of the stability tests, we also ran a coarser resolution

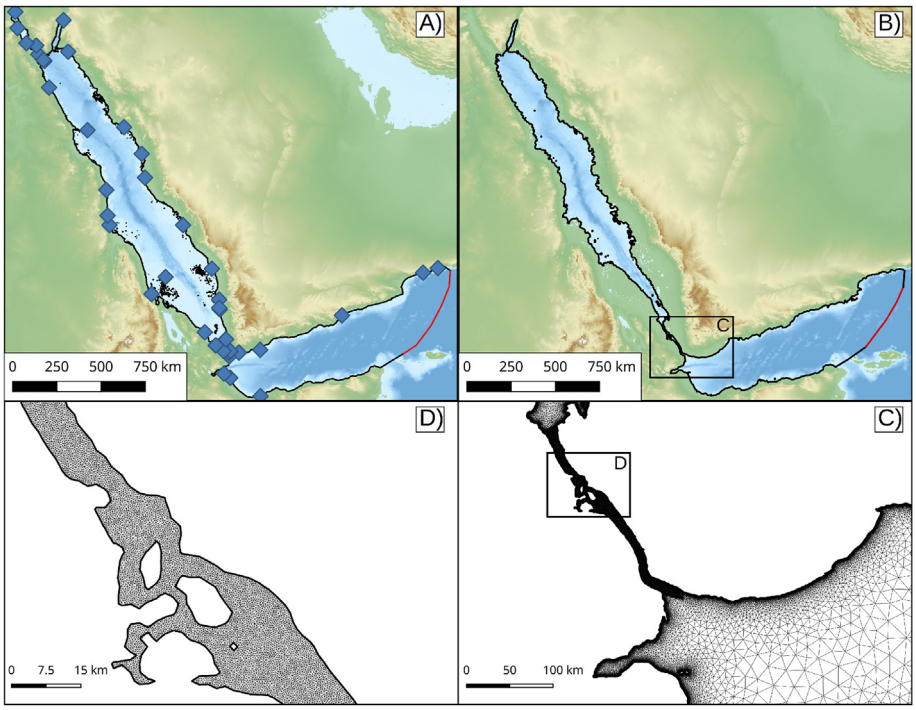

Fig. 3. Map showing tide gauge locations (see supplementary information for details) as blue diamonds, forced boundaries (red line) and no-flow boundaries (black) for the modern (A) and palaeo (B) domains. Close-ups of the mesh on the palaeo domain can be seen in C and D, as highlighted by the black rectangles. (For interpretation of the references to colour in this figure legend, the reader is referred to the Web version of this article.)

model to assess the impact of spatial resolution of the model. At open boundaries the flow is prescribed according to tidal harmonic data, using the FES 2014 data (Carrere et al., 2015). The simulation domain extends over the Gulf of Aden, in order to place the open boundary away from the region of interest and prevent boundary forcing from affecting the simulation predictive accuracy (Fig. 3A). For all models, the coastlines and sea bed boundaries were set to no-normal flow with a drag coefficient of 0.0025 [no units]. A uniform viscosity field was set as 1.0 (m^2s^{-1}) across the domain which ensures stability of the simulations (which have no turbulence parameterisation) but retains the ability to simulate and resolve large-scale eddies and complex currents. To further prevent instabilities forming along the forced boundary, an increased viscosity 100.0 m^2s^{-1} and Manning drag coefficient (0.25) were used at the forced boundary, linearly decreasing over a distance of 25 km to the background levels. All models simulated 60 days of forcing, starting from initial conditions of zero velocity and zero free surface elevation. The first 30 days were simulated to allow any transients induced by the initial conditions to subside and regular tidal patterns to be established. The final 30 days were used for all analyses presented here. Both the modern and palaeo models were forced along the boundary in the Gulf of Aden using FES 2014 data with eight principal tidal components, M_2, K_1, S_2, O_1, Q_1, P_1, N_2, and K_2. Together, these constitute the major tidal constituents in the Red Sea and Gulf of Aden.

The palaeo Red Sea model was set up to be as similar as possible to the modern, but replacing modern bathymetry-topography (Section 2.1) with the palaeo-topography at 21 ka from Lambeck et al. (2011) (see also Fig. 3B). The GIA formulation provides the change in sea level which when subtracted from the present bathymetry provides the palaeo water depths. The palaeoshoreline then corresponds to the 0 m palaeo-elevation contour. Similar to the modern set-up, the resolution of mesh varies from 1 km at the coastline to 25 km away from the coast, with an additional higher (500 m) resolution in the channel between the Bab al Mandab Strait and Hanish Sill to capture gyres and other small-scale flow structures in the area of interest (Fig. 3C and D). Islands smaller than the grid resolution were removed from the palaeoshoreline model. As for the modern tidal model, the open boundary was constructed across the entrance of the Gulf of Aden, where the shorelines were extended offshore to prevent instabilities arising from possible inconsistent forcing at the intersection of the open boundary and the shorelines. All meshes are constructed in gmsh (Geuzaine and Remacle, 2009) in UTM 37 N projection space. The modern mesh contains 53,326 elements, whilst the palaeo mesh contains 419,298 elements.

2.3. Simulation of movement

To simulate human movement, we use Lagrangian particles, which are passive virtual particles that move with the fluid flow. Particle movement was solved by a 4th-order guided search Runge-Kutta algorithm at each timestep of the tidal model. We inserted 100 randomly placed particles in three locations (300 detectors in total - see Fig. 7). The particles were added at 13 different times in the tidal cycle to examine how the timing of the tidal cycle influences drifting across the sea. Each of the 13 simulations with detectors was run for six days. Release times are shown with reference to free surface height near site 2 in Fig. 4. These particles represent floating objects and are carried by the instantaneous

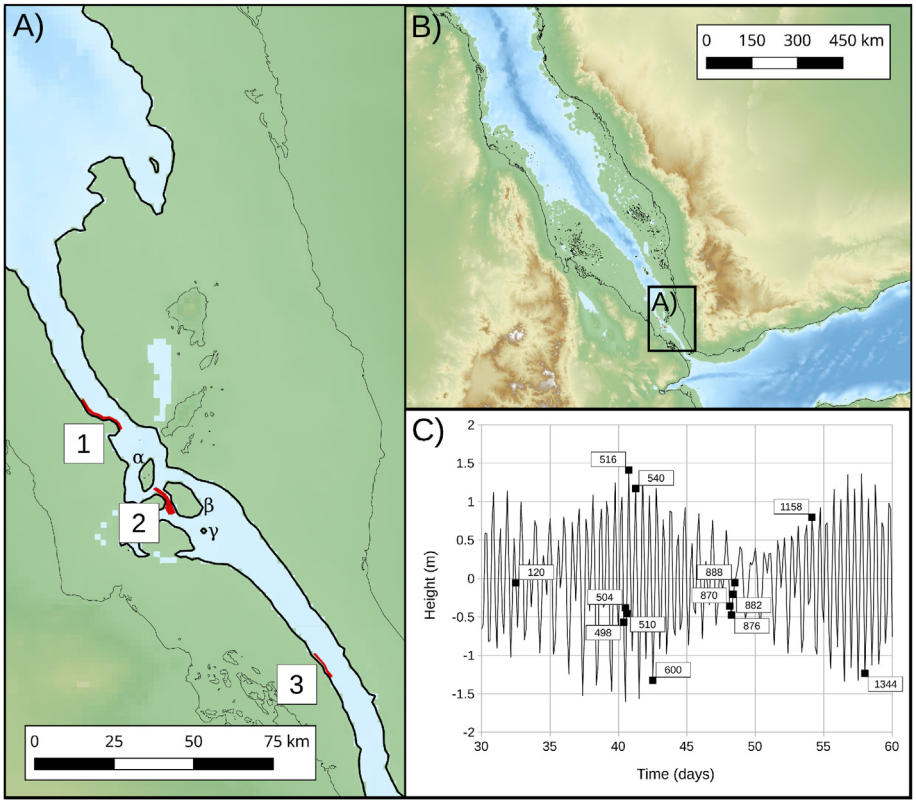

Fig. 4. A) Locations of particle release sites (labelled 1, 2 and 3), with islands in the centre of the straits labelled α, β, and γ. B) Overview map showing location of panel A. C) Water surface elevation from the palaeotidal model near site 3. Labelled square boxes show the time at which particles were released for the 13 simulations. Number refers to the output number of the primary simulation.

current; as such they simulate drifting of either rafts or individual humans, with no assisted movement (e.g. swimming or paddling). The percentage of particles that came within 100 m, 250 m or 500 m of the opposite shore were counted as having completed the journey within the six day period. These assumptions generate the minimum percentage of successful journeys. Any directed rafting or swimming would increase the reported percentage and as such the success rates are lower bounds, given the assumptions of no swimming or rafting.

3. Results

3.1. Tidal model validation

To assess model performance when simulating the LGM, we compared the model against tide gauge data in the Red Sea and Gulf of Aden using models of different spatial resolution. The model was run for a total of 60 days, with the first 30 days considered as 'spin-up', so that gauge comparisons could be carried out using 30 days of simulated tides. Data were then analysed at each tidal gauge and compared to the data collected. It should be noted that some tidal gauges only have 14 days of data from which to derive the tidal constituents. To compare the model against the tide gauges we use the method of Cummins and Oey (1997), whereby error, ξ, is calculated over the L tidal gauges as:

$$\xi = L^{-1} \sum D_L \tag{1}$$

$$D_L = \left[\frac{1}{2} \left(A_o^2 + A_m^2 \right) - A_o A_m \cos(\varphi_o - \varphi_m) \right]^{\frac{1}{2}}, \tag{2}$$

where A is tidal amplitude and φ is the phase of each tidal constituent in question. The subscript m refers to the model and o to observations. Table 1 shows the error calculation from each of the three modern day runs. In the modern day, the model has an error of 0.2–0.36 cm for M_2 and around 0.24 cm for K_1 across all 42 tidal stations, corresponding to a 0.08–1.5% and 2.2% error respectively according to equation (1). Fluidity appears to over predict the semi-diurnal components (S_2 and M_2) compared to tide gauges, but the diurnal components show an excellent agreement. Our results compare favourably to previous simulations of the Red Sea tides (Madah et al., 2015; Jarosz et al., 2005; Guo et al., 2018), with similar spatial patterns of M_2 and K_1 amplitudes and phases.

3.2. Tides at 21 ka

The simulation using the palaeobathymetry shows substantial changes to the modern tidal regime. The restriction in the Bab al Mandab straits causes a tidal blockage, preventing any substantial tidal current from entering the main Red Sea basin (Fig. 5). This results in a large M_2 amplitude in the central to northern section of the straits. Within the Red Sea itself, the M_2 amplitude is greatly reduced and we conclude that there would be little tidal range within the Sea at this time. The tidal amplitudes show an increase in M_2 to the south of the channel in the palaeo domain compared to the modern, with amplitudes peaking at over 1 m in the Gulf of Aden. There is a shift in the amphidromic point in the centre of the

Table 1
Model for different coastlines and model resolution for modern tidal simulations.

Model	M_2 error	S_2 error	K_1 error	O_1 error
GSHHS	0.36 cm (1.50%)	1.05 cm (12.73%)	0.24 cm (2.42%)	0.04 cm (0.71%)
0 m	0.20 cm (0.08%)	0.86 cm (11.01%)	0.24 cm (2.23%)	0.04 cm (0.55%)
0 m - coarse res	0.34 cm (1.41%)	1.02 cm (11.94%)	0.24 cm (2.20%)	0.04 cm (0.65%)

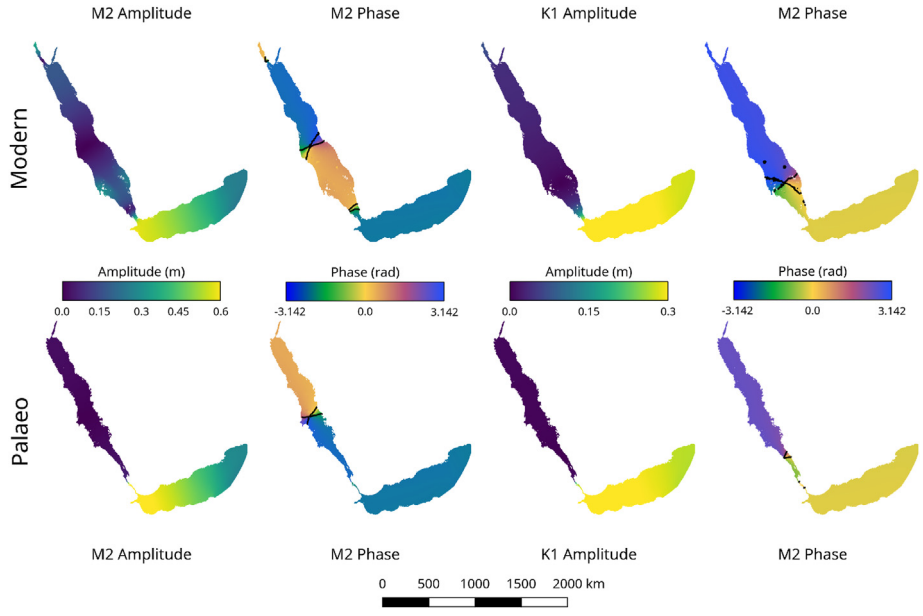

Fig. 5. Plots of amplitude and phase for the M_2 (left) and K_1 (right) for modern (top) and palaeo (bottom) domains. There is little change in K_1, but marked change of M_2 amplitude within the Red Sea itself, due to the restriction of the Bab al Mandab channel. (For interpretation of the references to colour in this figure legend, the reader is referred to the Web version of this article.)

Red Sea to the north and removal of the amphidromic points to the far north and south of the Red Sea, with a complete reversal of phase within the Red Sea. The phase in the Gulf of Aden remains similar to the modern day. The K_1 amplitude shows little change in both amplitude and phase, with a minor shift in the amphidromic point due to the restriction of the Red Sea and a slight decrease in K_1 amplitude in the far north in the palaeo compared to the modern domain. The large M_2 amplitude in the channel coincides with substantially increased currents, from a peak speed of around 0.75 m/s to just over 1 m/s. These peak currents also show a shift in position, from the southern end of the channel in the modern, to towards the northern half of the channel in the palaeo-domain, with a concentration of high speed around the islands in the central section of the channel.

Tidal velocities show a substantial shift in locations and amplitude. Here, we focus on the maximum flow speed over the 30 day simulation and on the Bab al Mandab channel. In the modern simulations, the peak velocities are seen in the southern section of the channel, peaking at around 0.7 m/s (Fig. 6). In general tidal flow is simple in the channel during the modern, with linear flow during ebb and flood tides. More complex flow patterns, including large-scale gyres, form during slack tide, where outgoing flow occurs along the coast and flow is into the Red Sea in the centre of the channel. There is a clear reduction in the lee of islands and over shallow areas of reef, with more complex flow patterns in those regions as is to be expected. In the palaeo domain, the highest tidal velocities are now in the northern section, just south of where the channel opens into the Red Sea. The reconstruction indicates the presence of a number of islands here where the tidal flow is accelerated. Peak speeds are over 1 m/s, with the peak flow direction along the seaway, either to the south or the north. Further south in the straits, the flow speed is lower, but there is a peak of just over 0.5 m/s. In addition, the simulation reveals a number of gyres and other complex flow structures, with a large gyre highlighted in the average flow direction (Fig. 6C).

3.3. Drift locations

To assess the likelihood of traversing the Bab al Mandab channel without any extensive need to paddle rafts, we simulated how passive objects would drift in the tidal currents. Analysing the results over the 13 simulations for each site (1300 particles per site in total) shows that the percentage of success is dependant on site and time of journey start (Table 2). Sites 1 and 2 are the most successful for completing the journey as Site 3 has no successful journeys as the tidal flow is relatively simple with very little across channel flow. In contrast, sites 1 and 2 show complex flow and as such show very different rates of success of crossing the sea here. Using the 500 m distance threshold as a benchmark, Site 1 has an average success rate of 16.4% whereas Site 2 is 11.45%. The average crossing time for the journey at Site 2 is only slightly lower at 3.8 days compared to 3.9 days. The shortest average time for the journey is from Site 1 and takes 2.9 days on average with 19% of particles being successful in making the crossing. The quickest time for a single journey is 1.4 days from Site 2.

The tidal conditions at the time of starting the journey have a large impact on the success rate. The most successful time for release was between days 40 and 45 with up to 42 of 200 particles coming within 500 m of the opposite shoreline from sites 1 and 2. The least successful time was during the neap tide (around day 48) with a maximum journey time of 4.6 days. The maximum number of successful journeys was 13 from 200 particles from sites 1 and 2. The rapid currents during the spring tide clearly increases the chances of reaching the opposing shoreline.

In addition, site 2 is close to two large islands (α and β) in the palaeo-topography. It is therefore very possible to 'island-hop' using the tidal flow from that site (see pathways in Fig. 7). The flow patterns at these sites are very complex however. In particular particles released from site 1 were often trapped in a large gyre to the south of the release site, but north-west of island α (Fig. 7). Similar pathways also occurred from site 2, but the particles were

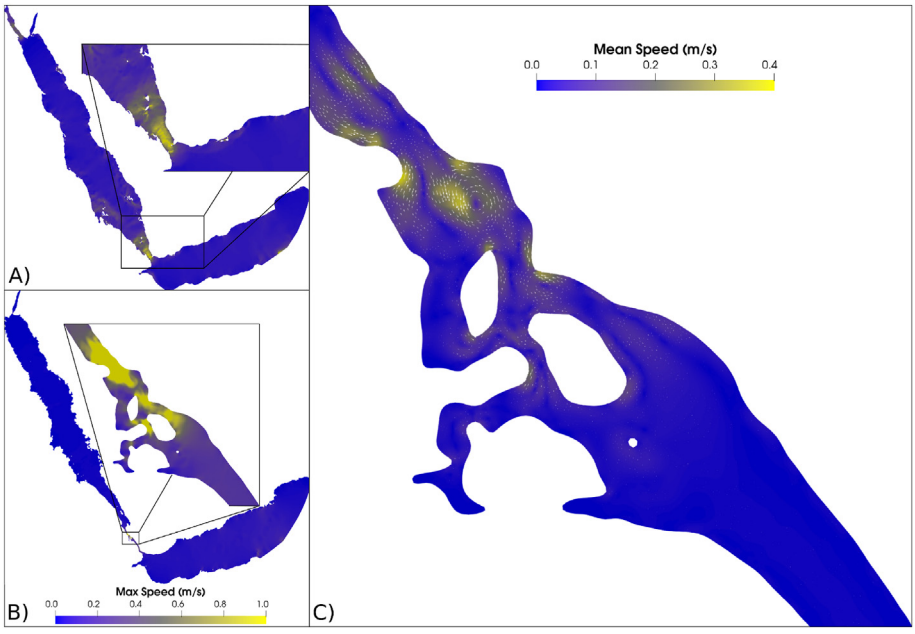

Fig. 6. Plots of maximum tidal flow speed over the 30 simulated days. Upper-left (A) is the modern Red Sea, with the inset showing the Bab al Mandab channel. Lower-left (B) is the palaeo domain, again with inset showing the straits. Modern flow is much higher within the Red Sea itself, but flow in the straits is much higher (factor of 2) in the palaeo domain due to the restriction. Panel C shows the mean tidal flow over 30 days at 21 ka. Note the clear eddy formation in the residual tidal flow. (For interpretation of the references to colour in this figure legend, the reader is referred to the Web version of this article.)

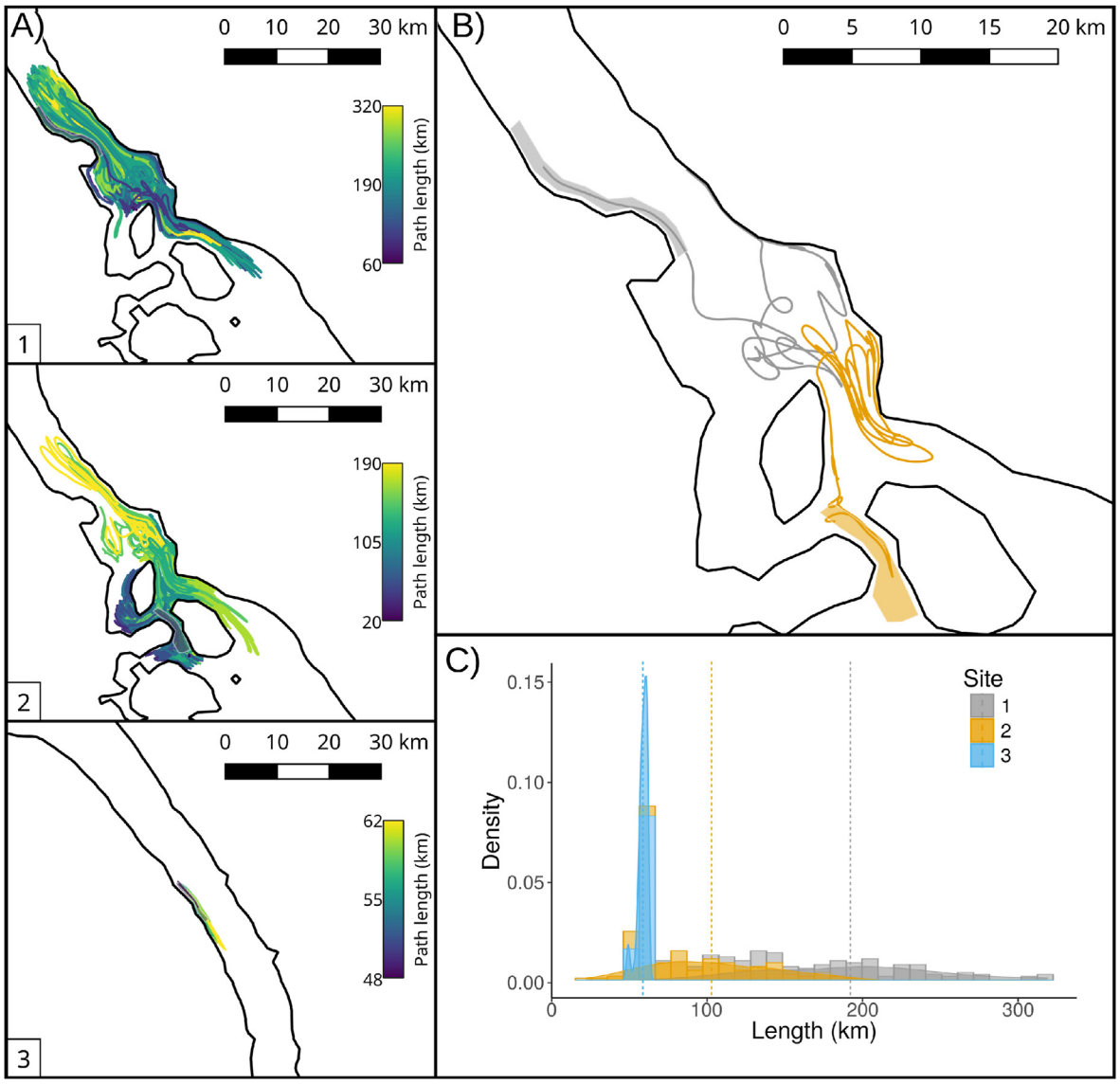

Fig. 7. Complete set of pathways for each release site from simulation 498 (A). Colour shows the length of each pathway in kilometres. Note the change in colour scale for each site. Two example pathways that are successful from sites 1 and 2 are shown in B). Colour corresponds to the key in C). The distributions of lengths (over the whole 6 days simulated time) are shown in C). The vertical dotted line indicates the mean length. Colour indicates which site the particle was released from. (For interpretation of the references to colour in this figure legend, the reader is referred to the Web version of this article.)

more often accelerated past the offshore gyre west of β and hence could travel north over 20 km from the start location.

Site 3, at the southern end of the channel shows a very simple tidal flow, with a tight closure of the tidal ellipse resulting in a simple 'back-and-forth' motion of the particles (not shown). With assisted sailing, the tidal currents, though relatively strong for short periods, would move vessels to the north or south in a predictable way and given the overall relatively low tidal velocities in this region would make the crossing very straightforward.

The starting sites showed considerable differences when looking at how far particles travelled (Fig. 7C). Release from Site 1 resulted in particles travelling 60 and 320 km (over the six days), which equates to average speeds of 0.11 m/s to 0.61 m/s. Similarly, Site 2 resulted in distances of 20–190 km (0.039 m/s to 0.37 m/s average speeds). Both resulted in very complex pathways which often traversed the gyre seen in the average velocity data (Fig. 6C). Both sites showed a wide spread of possible distances crossed, but a reasonable percentage did result in a successful crossing of the channel. In contrast Site 3 shows a narrow range of distances travelled from 48 to 62 km. This is a result of the very simple oscillatory tidal flow and the low speed of that flow. Average speeds of the tidal current here are 0.09 m/s to 0.12 m/s.

The results indicate that crossing in the region where tidal currents are strongest would be somewhat unpredictable, but a substantial proportion of particles did land on the opposite coast without any recourse to directed rafting or swimming. Further south, the tidal currents are very predictable, but preclude simply rafting across the straits. To cross here would require directed rafting or swimming of some kind.

4. Discussion

One of the arguments against the southern dispersal route is that the Bab al Mandab straits were never dry and therefore modern humans would have required a sea crossing even at periods of lowest Pleistocene sea level. Here, we show that for long

Table 2
Number of particles that come within 500 m of the opposing shoreline, for each site and simulation. Simulation names refer to those on Fig. 4. Average time is for all successful journeys from that site. Site three is not shown as no particles came within 500 m of the opposing shoreline.

Simulation	Site Number	Number crossed	Average Time (days)
120	1	20	4.33
	2	19	3.09
	Total	39	
498	1	34	3.58
	2	8	3.35
	Total	42	
504	1	28	3.83
	2	6	4.80
	Total	34	
510	1	11	3.43
	2	18	3.11
	Total	29	
516	1	18	3.92
	2	11	3.46
	Total	29	
540	1	22	4.02
	2	9	3.93
	Total	31	
600	1	20	4.21
	2	20	3.48
	Total	40	
870	1	3	3.83
	2	7	4.61
	Total	10	
876	1	3	3.37
	2	6	4.58
	Total	9	
882	1	4	4.17
	2	5	4.38
	Total	9	
888	1	3	4.80
	2	10	3.84
	Total	13	
1158	1	19	2.88
	2	20	3.58
	Total	39	
1344	1	28	4.02
	2	10	3.12
	Total	38	

periods of the Pleistocene sea-level cycle, a narrow channel would have extended for 150 km from the present-day mouth of the Bab al Mandab to the Hanish Sill region with clear intervisibility between the opposing shores. We also show that the tidal currents in this palaeo-channel, though complex, would have allowed for successful sea crossings of the simplest kind – by passive drifting or rafting – and that up to 32% of journeys of this kind in the central and northern section of the channel reached the opposite coastline. The flow rates from tides are highest in the centre of the straits (Fig. 6) at just over 1 m/s. In the shallow regions, the tidal flow is much slower (0.1–0.5 m/s). Humans can stand without difficulty in water of up to 1 m depth at these flow speeds (Jonkman et al., 2008). To cross the straits in this way would have needed knowledge of the current via observation, but given the strong arguments of early humans living along the coastline in this region (Bailey, 2010; Walter et al., 2000; Inglis et al., 2019b), it is not unreasonable to assume that they would acquire this knowledge.

The numerical modelling presented here used three sites from which to randomly place starting particles. These three sites were chosen to represent three obvious pathways across the straits. Site 1 is the narrowest part of the straits in this reconstruction. However, it has the most complex tidal flow patterns of the three sites, with the occurrence of a large gyre to the south which traps particles for many days. Site 2 was placed near the island chain, with two large islands α and β, which would make an "island-hopping" approach possible. Here, we find that the flow paths of particles is complex, but does intersect with both α and β islands. With careful choice of where to launch it would be a relatively simple matter to raft across the channel here; launching at slack tide and reaching the next island is entirely feasible. To test this idea we performed two further simulations. Particles were released to the west of the β island at release times 120 and 1158. It was found that no particles reached the opposite side of the straits at time 120, but 5% did at time 1158 (see supplementary information). Island hopping is therefore a clear possibility, but more work would be required to fully examine this idea. Phylogenetic interpretation of mtDNA in modern baboon populations (*Papio hamadryas*) living on either side of the southern Red Sea suggests movement across the southern Red Sea on at least two occasions during the late Pleistocene, presumably by accidental drifting (Kopp et al., 2014), which we have shown is possible within a few days. Our results also support the conclusions of the agent-based modelling approach of Hölzchen et al. (2022), but with the addition of high-resolution palaeotopographic and palaeooceanographic detail not available to them.

Site 3 is perhaps the most interesting as the tidal currents are very simple, with a clear north-south oscillating direction. Passive drifting here is not possible, but directed rafting or swimming would be much easier as the maximum tidal current in a given cycle is as low as 0.2 m/s. The strait is also narrow, around 10 km. Sustained powered travel at 0.5 m/s would mean reaching the opposite bank in around 5–6 h, not accounting for the drift caused by the weak tidal current, which would be roughly orthogonal to the direction of travel. In comparison, the English Channel is 32 km wide and is swum in an average time of just over 13.5 h, giving an average speed of 0.66 m/s (Dover.UK.com, 2022). Moreover, the contrast between site 3 and sites 1 and 2 shows that crossing the southern Red Sea would be feasible, regardless of the exact nature of the tidal flow, for long durations during sea-level lowstands. It would require further work to establish at what sea level crossing becomes difficult without powered navigation as the details of the complex flow patterns would be a strong determinant in that assessment.

4.1. Model uncertainties

The model presented here contains a number of uncertainties. They do not affect the overall conclusions, but deserve comment as factors that offer scope for refinement of particle motions. Firstly, the model contains no simulation of tidal inundation (also known as wetting and drying). This is largely due to the relatively coarse resolution of the bathymetry/topography and hence the mesh near the coastlines. Secondly, the palaeo-bathymetric reconstruction does not account for any coastal geomorphological changes resulting from coastal erosion or offshore sedimentation. It is based on modern topography with relative sea level change accounted for. Existing research suggests that the effect of such geomorphological processes along the coastlines of the southern Red Sea is relatively minor in comparison with eustatic, GIA and tectonic modifications of shoreline position (Rasul et al., 2019). Nevertheless, the model we have presented here is open to further refinement in the light of more detailed investigation of shoreline processes. Finally, the model does not include any ocean or wind-driven currents. We have focused exclusively on tidal currents. This is because tidal currents and are inherently predictable and obvious to the human observer, and observation over months or years will lead to an understanding of their behaviour. Wind and ocean currents are less easily predicted and hence add additional unpredictability to the currents. Our focus here was predictable

currents. Adding ocean and wind-driven currents and assessing the impact would be interesting future work.

5. Conclusions

Blending palaeo-topographic/bathymetric reconstructions with palaeotidal modelling shows that, although tidal currents were faster during glacial maxima than today, the crossing distances were much shorter. Even without any kind of powered navigation, up to 32% of passive Langrangian particles came within 500 m of the opposing shoreline (the effective threshold for defining a successful landfall). Once the ability to notice the changes in tidal currents is factored in, the crossing, though challenging, is most certainly feasible. Anyone crossing the southern Red Sea at the time would have sight of the opposing shoreline and if they commenced the crossing at the right time and location they would have encountered very little north-south flow for much of the duration. If powered crossing is factored in, the crossing at the southernmost part of the channel would be easiest and would take 5–6 h at a reasonable swimming speed. We conclude that although the tidal currents in the LGM are likely to have been faster and more complex than today, they would not have presented an obstacle to crossing the Red Sea at sea-level minima by either drifting passively or rafting. These results do not provide definitive proof in favour of human crossings of the southern Red Sea during Pleistocene low sea levels. But they demonstrate that the southern crossing can no longer be dismissed on the grounds of difficulty, distance, dangerous sea conditions, or risk of failure.

Credit author contributions

Jon Hill: Conceptualization, Methodology, Visualization, Formal analysis, Writing – original draft, Writing- Reviewing and Editing **Alexandros Avdis**: Data curation, Validation, Conceptualization, Methodology. **Geoff Bailey**: Writing- Reviewing and Editing, Writing – original draft, Conceptualization. **Kurt Lambeck**: Writing- Reviewing and Editing, Writing – original draft, Conceptualization, Resources

Declaration of competing interest

The authors declare that they have no known competing financial interests or personal relationships that could have appeared to influence the work reported in this paper.

Data availability

Data will be made available on request.

Acknowledgements

This project was undertaken on the Viking Cluster, which is a high performance compute facility provided by the University of York. We are grateful for computational support from the University of York High Performance Computing service, Viking and the Research Computing team. We also thank Robyn Inglis for comments on an earlier draft. The project originated in field investigations in the southern Red Sea supported by NERC under its EFCHED programme and the ERC under the Ideas Programme of the 7th Framework Programme as Advanced Grant 269586DISPERSE. This is DISPERSE Publication No. 66. We thank an anonymous reviewer and Jerry Mitrovica for helpful and constructive comments.

Appendix A. Supplementary data

Supplementary data to this article can be found online at https://doi.org/10.1016/j.quascirev.2022.107719.

References

Abbate, E., Sagri, M., 2012. Early to Middle Pleistocene Homo dispersals from Africa to Eurasia: geological, climatic and environmental constraints. Quat. Int.: the journal of the International Union for Quaternary Research 267, 3–19. https://doi.org/10.1016/j.quaint.2011.02.043.

Alimen, M.H., 1975. Les 'isthmes' hispano-marocain et Siculo-Tunisien aux temps acheuléens. L'anthropologie 79, 399–436.

Allen, J., O'Connell, J.F., 2008. Getting from Sunda to Sahul. https://doi.org/10.22459/ta29.06.2008.02.

Antonioli, F., Chiocci, F.L., Anzidei, M., Capotondi, L., Casalbore, D., Magri, D., Silenzi, S., 2017. The central mediterranean. In: Submerged Landscapes of the European Continental Shelf. John Wiley & Sons, Ltd, Oxford, UK, pp. 341–376. https://doi.org/10.1002/9781118927823.ch13.

Antonioli, F., Lo Presti, V., Morticelli, M.G., Bonfiglio, L., Mannino, M.A., Palombo, M.R., Sannino, G., Ferranti, L., Furlani, S., Lambeck, K., Canese, S., Catalano, R., Chiocci, F.L., Mangano, G., Scicchitano, G., Tonielli, R., 2016. Timing of the emergence of the Europe–Sicily bridge (40–17 cal ka BP) and its implications for the spread of modern humans. Geological Society, London, Special Publications 411, 111–144. https://doi.org/10.1144/SP411.1, 10.1144/SP411.1.

Augustin, N., Devey, C.W., van der Zwan, F.M., 2019. A modern view on the red sea rift: tectonics, volcanism and salt blankets. In: Rasul, N.M.A., Stewart, I.C.F. (Eds.), Geological Setting, Palaeoenvironment and Archaeology of the Red Sea. Springer International Publishing, Cham, pp. 37–52. https://doi.org/10.1007/978-3-319-99408-6_3.

Austin, R.M., 1991. Modelling Holocene tides on the NW European continental shelf. Terra. Nova 3, 276–288. https://doi.org/10.1111/j.1365-3121.1991.tb00145.x.

Avdis, A., Candy, A.S., Hill, J., Kramer, S.C., Piggott, M.D., 2018. Efficient unstructured mesh generation for marine renewable energy applications. Renew. Energy 116, 842–856. https://doi.org/10.1016/j.renene.2017.09.058.

Bailey, G., 2010. The red sea, coastal landscapes, and hominin dispersals. In: Petraglia, M.D., Rose, J.I. (Eds.), The Evolution of Human Populations in Arabia: Paleoenvironments, Prehistory and Genetics. Springer Netherlands, Dordrecht, pp. 15–37. https://doi.org/10.1007/978-90-481-2719-1_2.

Bailey, G., 2013. Early seafaring and the archaeology of submerged landscapes. Eurasian Prehistory 10, 99–114.

Bailey, G., 2015. The evolution of the red sea as a human habitat during the quaternary period. In: Rasul, N.M.A., Stewart, I.C.F. (Eds.), The Red Sea: the Formation, Morphology, Oceanography and Environment of a Young Ocean Basin. Springer Berlin Heidelberg, Berlin, Heidelberg, pp. 599–614. https://doi.org/10.1007/978-3-662-45201-1_34.

Bailey, G., Carrion, J.S., Fa, D.A., Finlayson, C., Finlayson, G., Rodriguez-Vidal, J., 2008. The coastal shelf of the Mediterranean and beyond: corridor and refugium for human populations in the Pleistocene. Quat. Sci. Rev. 27, 2095–2099.

Bailey, G., King, G., Sturdy, D., 1993. Active tectonics and land-use strategies: a Palaeolithic example from northwest Greece. Antiquity 67, 292–312. https://doi.org/10.1017/S0003598X00045361.

Bailey, G.N., Devès, M.H., Inglis, R.H., Meredith-Williams, M.G., Momber, G., Sakellariou, D., Sinclair, A.G.M., Rousakis, G., Al Ghamdi, S., Alsharekh, A.M., 2015. Blue Arabia: Palaeolithic and underwater survey in SW Saudi Arabia and the role of coasts in Pleistocene dispersals. Quat. Int.: the journal of the International Union for Quaternary Research 382, 42–57. https://doi.org/10.1016/j.quaint.2015.01.002.

Bailey, G.N., Flemming, N.C., King, G.C.P., Lambeck, K., Momber, G., Moran, L.J., Al-Sharekh, A., Vita-Finzi, C., 2007. Coastlines, submerged landscapes, and human evolution: the red sea basin and the farasan islands. J. I. Coast Archaeol. 2, 127–160. https://doi.org/10.1080/15564890701623449.

Bailey, G.N., Reynolds, S.C., King, G.C.P., 2011. Landscapes of human evolution: models and methods of tectonic geomorphology and the reconstruction of hominin landscapes. J. Hum. Evol. 60, 257–280. https://doi.org/10.1016/j.jhevol.2010.01.004.

Bednarik, R.G., 1999. Maritime navigation in the lower and Middle palaeolithic. Comptes Rendus Acad. Sci. - Ser. IIA Earth Planet. Sci. 328, 559–563. https://doi.org/10.1016/S1251-8050(99)80139-6.

Beyin, A., 2006. The Bab Al Mandab vs the Nile-Levant: an Appraisal of the Two Dispersal Routes for Early Modern Humans Out of Africa. https://doi.org/10.1007/s10437-006-9005-2.

Beyin, A., 2011. Upper Pleistocene human dispersals out of Africa: a review of the current state of the debate. Int. J. Evol. Biol. 2011, 615094. https://doi.org/10.4061/2011/615094.

Bird, M.I., Beaman, R.J., Condie, S.A., Cooper, A., Ulm, S., Veth, P., 2018. Palaeogeography and voyage modeling indicates early human colonization of Australia was likely from Timor-Roti. Quat. Sci. Rev. 191, 431–439. https://doi.org/10.1016/j.quascirev.2018.04.027.

Boivin, N., Fuller, D.Q., Dennell, R., Allaby, R., Petraglia, M.D., 2013. Human dispersal across diverse environments of Asia during the upper Pleistocene. Quat. Int.: the journal of the International Union for Quaternary Research 300, 32–47. https://doi.org/10.1016/j.quaint.2013.01.008.

Bolus, M., 2015. Dispersals of early humans: adaptations, frontiers, and new territories. In: Henke, W., Tattersall, I. (Eds.), Handbook of Paleoanthropology. Springer Berlin Heidelberg, Berlin, Heidelberg, pp. 2371–2400. https://doi.org/10.1007/978-3-642-39979-4_83.

Boone, S.C., Balestrieri, M.L., Kohn, B., 2021. Thermo-tectonic imaging of the Gulf of aden-red sea rift systems and afro-arabian hinterland. Earth Sci. Rev. 222, 103824. https://doi.org/10.1016/j.earscirev.2021.103824.

Borreggine, M., Powell, E., Pico, T., Mitrovica, J.X., Meadow, R., Tryon, C., 2022. Not a bathtub: a consideration of sea-level physics for archaeological models of human migration. J. Archaeol. Sci. 137, 105507. https://doi.org/10.1016/j.jas.2021.105507.

Bosworth, W., Taviani, M., Rasul, N.M.A., 2019. Neotectonics of the red sea, Gulf of Suez and Gulf of aqaba. In: Rasul, N.M.A., Stewart, I.C.F. (Eds.), Geological Setting, Palaeoenvironment and Archaeology of the Red Sea. Springer International Publishing, Cham, pp. 11–35. https://doi.org/10.1007/978-3-319-99408-6_2.

Broodbank, C., 2014. So…What? Does the paradigm currently want to budge so much? J. Mediterr. Archaeol. 27, 267–272.

Brumm, A., Jensen, G.M., van den Bergh, G.D., Morwood, M.J., Kurniawan, I., Aziz, F., Storey, M., 2010. Hominins on Flores, Indonesia, by one million years ago. Nature 464, 748–752. https://doi.org/10.1038/nature08844.

Canals, M., Cacho, I., Carozza, L., Casamor, J.L., Lastras, G., Sanchez, A., 2017. The western mediterranean sea. Submerged Landscapes of the European Continental Shelf: Quaternary Paleoenvironments 301–340.

Carrere, L., Lyard, F., Cancet, M., Guillot, A., 2015. FES 2014, a new tidal model on the global ocean with enhanced accuracy in shallow seas and in the arctic region. In: EGU General Assembly. European Geophysical Union.

Carter, R.A., 2010. The Social and Environmental Context of Neolithic Seafaring in the Persian Gulf. The Global Origins and Development of Seafaring, pp. 191–202.

Castagnino Berlinghieri, E.F., Antonioli, F., Bailey, G., 2020. Italy: the archaeology of palaeoshorelines, coastal caves and seafaring connections. In: Bailey, G., Galanidou, N., Peeters, H., Jöns, H., Mennenga, M. (Eds.), The Archaeology of Europe's Drowned Landscapes. Springer International Publishing, Cham, pp. 321–340. https://doi.org/10.1007/978-3-030-37367-2_16.

Cathles, L.M., 1975. The Viscosity Ofthe Earth's Mantle. The Princeton University library chronicle.

Chiocci, F.L., Casalbore, D., Marra, F., Antonioli, F., Romagnoli, C., 2017. relative sea level rise, palaeotopography and transgression velocity on the continental shelf. In: Bailey, G.N., Harff, J., Sakellariou, D. (Eds.), Under the Sea: Archaeology and Palaeolandscapes of the Continental Shelf. Springer International Publishing, Cham, pp. 39–51. https://doi.org/10.1007/978-3-319-53160-1_3.

Clarkson, C., Jacobs, Z., Marwick, B., Fullagar, R., Wallis, L., Smith, M., Roberts, R.G., Hayes, E., Lowe, K., Carah, X., Florin, S.A., McNeil, J., Cox, D., Arnold, L.J., Hua, Q., Huntley, J., Brand, H.E.A., Manne, T., Fairbairn, A., Shulmeister, J., Lyle, L., Salinas, M., Page, M., Connell, K., Park, G., Norman, K., Murphy, T., Pardoe, C., 2017. Human occupation of northern Australia by 65,000 years ago. Nature 547, 306–310. https://doi.org/10.1038/nature22968.

Collins, D.S., Avdis, A., Allison, P.A., Johnson, H.D., Hill, J., Piggott, M.D., 2018. Controls on tidal sedimentation and preservation: insights from numerical tidal modelling in the late oligocene–miocene south China sea, southeast Asia. Sedimentology 95, 529. https://doi.org/10.1111/sed.12474.

Collins, D.S., Avdis, A., Allison, P.A., Johnson, H.D., Hill, J., Piggott, M.D., Amir Hassan, M.H., Damit, A.R., 2017. Tidal dynamics and mangrove carbon sequestration during the oligo–miocene in The south China sea. Nat. Commun. 8. https://doi.org/10.1038/ncomms15698 ncomms15698.

Cummins, P.F., Oey, L.Y., 1997. Simulation of barotropic and baroclinic tides off northern British columbia. J. Phys. Oceanogr. 27, 762–781. https://doi.org/10.1175/1520-0485(1997)027¡0762:SOBABT¿2.0.CO;2.

Davies, H.S., Green, J.A., Duarte, J.C., 2020. Back to the future II: tidal evolution of four supercontinent scenarios. Earth System Dynamics 11, 291–299. https://doi.org/10.5194/esd-2019-61.

Dennell, R., 2008. The Palaeolithic Settlement of Asia. Cambridge University Press.

Dennell, R.W., Louys, J., O'Regan, H.J., Wilkinson, D.M., 2014. The origins and persistence of Homo floresiensis on Flores: biogeographical and ecological perspectives. Quat. Sci. Rev. 96, 98–107. https://doi.org/10.1016/j.quascirev.2013.06.031.

Dover.UK.com, 2022. Swimming the English Channel. https://www.dover.uk.com/channel-swimming/. (Accessed 14 January 2022). Accessed.

Durrani, N., 2005. The Tihamah coastal plain of South-West Arabia in its regional context, c.6000 BC - ad 600. In: Society for Arabian Studies Monographs. Archaeopress, Oxford, England.

Egbert, G.D., Ray, R.D., Bills, B.G., 2004. Numerical modeling of the global semidiurnal tide in the present day and in the last glacial maximum. J. Geophys. Res. 109. https://doi.org/10.1029/2003jc001973.

Farrell, W.E., Clark, J.A., 1976. On postglacial sea level. Geophys. J. Int. 46, 647–667. https://doi.org/10.1111/j.1365-246X.1976.tb01252.x.

Ferentinos, G., Gkioni, M., Geraga, M., Papatheodorou, G., 2012. Early seafaring activity in the southern ionian islands, mediterranean sea. J. Archaeol. Sci. 39, 2167–2176. https://doi.org/10.1016/j.jas.2012.01.032.

Flemming, N.C., Harff, J., Moura, D., Burgess, A., Bailey, G.N., 2017. Submerged Landscapes of the European Continental Shelf: Quaternary Paleoenvironments. John Wiley & Sons.

Gaffney, D., 2021. Pleistocene water crossings and adaptive flexibility within the Homo genus. J. Archaeol. Res. 29, 255–326. https://doi.org/10.1007/s10814-020-09149-7.

Galanidou, N., 2014. Advances in the Palaeolithic and Mesolithic archaeology of Greece for the new millennium. The Pharos of Alpha Omega Alpha-Honor Medical Society. Alpha Omega Alpha 20, 1–40.

Geuzaine, C., Remacle, J.F., 2009. Gmsh: a 3-D finite element mesh generator with built-in pre- and post-processing facilities. Int. J. Numer. Methods Eng. 79, 1309–1331. https://doi.org/10.1002/nme.2579.

Grant, K.M., Rohling, E.J., Ramsey, C.B., Cheng, H., Edwards, R.L., Florindo, F., Heslop, D., Marra, F., Roberts, A.P., Tamisiea, M.E., Williams, F., 2014. Sea-level variability over five glacial cycles. Nat. Commun. 5, 5076. https://doi.org/10.1038/ncomms6076, 10.1038/ncomms6076.

Groucutt, H.S., Grün, R., Zalmout, I.A.S., Drake, N.A., Armitage, S.J., Candy, I., Clark-Wilson, R., Louys, J., Breeze, P.S., Duval, M., Buck, L.T., Kivell, T.L., Pomeroy, E., Stephens, N.B., Stock, J.T., Stewart, M., Price, G.J., Kinsley, L., Sung, W.W., Alsharekh, A., Al-Omari, A., Zahir, M., Memesh, A.M., Abdulshakoor, A.J., Al-Masari, A.M., Bahameem, A.A., Al Murayyi, K.M.S., Zahrani, B., Scerri, E.L.M., Petraglia, M.D., 2018. Homo sapiens in Arabia by 85,000 years ago. Nature ecology & evolution 2, 800–809. https://doi.org/10.1038/s41559-018-0518-2.

Groucutt, H.S., Petraglia, M.D., Bailey, G., Scerri, E.M.L., Parton, A., Clark-Balzan, L., Jennings, R.P., Lewis, L., Blinkhorn, J., Drake, N.A., Breeze, P.S., Inglis, R.H., Devès, M.H., Meredith-Williams, M., Boivin, N., Thomas, M.G., Scally, A., 2015. Rethinking the dispersal of Homo sapiens out of Africa. Evol. Anthropol. 24, 149–164. https://doi.org/10.1002/evan.21455.

Guo, D., Kartadikaria, A., Zhan, P., Xie, J., Li, M., Hoteit, I., 2018. Baroclinic tides simulation in the red sea: comparison to observations and basic characteristics. J. Geophys. Res. C Oceans 123, 9389–9404. https://doi.org/10.1029/2018jc013970.

Haigh, I.D., Pickering, M.D., Green, J.M., Arbic, B.K., Arns, A., Dangendorf, S., Hill, D.F., Horsburgh, K., Howard, T., Idier, D., Jay, D.A., 2020. The tides they are A-changin': a comprehensive review of past and future nonastronomical changes in tides, their driving mechanisms, and future implications. Rev. Geophys. 58, 1.

Hausmann, N., Meredith-Williams, M., Laurie, E., 2021. Shellfish resilience to prehistoric human consumption in the southern Red Sea: variability in Conomurex fasciatus across time and space. Quat. Int.: the journal of the International Union for Quaternary Research 584, 20–32. https://doi.org/10.1016/j.quaint.2020.04.034.

Hill, J., Piggott, M.D., Ham, D.A., Popova, E.E., Srokosz, M.A., 2012. On the performance of a generic length scale turbulence model within an adaptive finite element ocean model. Ocean Model. 56, 1–15.

Hill, J., Popova, E.E., Ham, D.A., Piggott, M.D., Srokosz, M., 2014. Adapting to life: ocean biogeochemical modelling and adaptive remeshing. Ocean Sci. 10, 323–343. https://doi.org/10.5194/os-10-323-2014.

Hinton, A.C., 1995. Holocene tides of the Wash, U.K.: the influence of water-depth and coastline-shape changes on the record of sea-level change. Mar. Geol. 124, 87–111. https://doi.org/10.1016/0025-3227(95)00034-V.

Hölzchen, E., Hertler, C., Willmes, C., Anwar, I.P., Mateos, A., Rodríguez, J., Berndt, J.O., Timm, I.J., 2022. Estimating crossing success of human agents across sea straits out of Africa in the Late Pleistocene. Palaeogeogr. Palaeoclimatol. Palaeoecol. 590, 110845. https://doi.org/10.1016/j.palaeo.2022.110845.

Howitt-Marshall, D., Runnels, C., 2016. Middle Pleistocene sea-crossings in the eastern mediterranean? J. Anthropol. Archaeol. 42, 140–153. https://doi.org/10.1016/j.jaa.2016.04.005.

Inglis, R.H., Bosworth, W., Rasul, N.M.A., Al-Saeedi, A.O., Bailey, G.N., 2019a. Investigating the palaeoshorelines and coastal archaeology of the southern red sea. In: Rasul, N.M.A., Stewart, I.C.F. (Eds.), Geological Setting, Palaeoenvironment and Archaeology of the Red Sea. Springer International Publishing, Cham, pp. 553–581. https://doi.org/10.1007/978-3-319-99408-6_25.

Inglis, R.H., Fanning, P.C., Stone, A., Barfod, D.N., Sinclair, A., Chang, H.C., Alsharekh, A.M., Bailey, G., 2019b. Paleolithic artifact deposits at Wadi Dabsa, Saudi Arabia: a multiscalar geoarchaeological approach to building an interpretative framework. Geoarchaeology 34, 272–294. https://doi.org/10.1002/gea.21723.

Jarosz, E., Blain, C.A., Murray, S.P., Inoue, M., 2005. Barotropic tides in the Bab el Mandab Strait—numerical simulations. Continent. Shelf Res. 25, 1225–1247. https://doi.org/10.1016/j.csr.2004.12.017.

Johnston, P., 1993. The effect of spatially non-uniform water loads on prediction of sea-level change. Geophys. J. Int. 114, 615–634. https://doi.org/10.1111/j.1365-246X.1993.tb06992.x.

Jonkman, S.N., Vrijling, J.K., Vrouwenvelder, A.C.W.M., 2008. Methods for the estimation of loss of life due to floods: a literature review and a proposal for a new method. Nat. Hazards 46, 353–389. https://doi.org/10.1007/s11069-008-9227-5.

Joordens, J.C.A., Dupont-Nivet, G., Feibel, C.S., Spoor, F., Sier, M.J., van der Lubbe, J.H.J.L., Nielsen, T.K., Knul, M.V., Davies, G.R., Vonhof, H.B., 2013. Improved age control on early Homo fossils from the upper Burgi Member at Koobi Fora, Kenya. J. Hum. Evol. 65, 731–745. https://doi.org/10.1016/j.jhevol.2013.09.002.

Kaczanowska, M., Kozłowski, J., 2014. The Aegean Mesolithic: material culture, chronology, and networks of contact. Eurasian Prehistory 11.

Kiki Kuijjer, E., Haigh, I.D., Marsh, R., Helen Farr, R., 2022. Changing tidal dynamics and the role of the marine environment in the maritime migration to Sahul. PaleoAnthropology 134–148doi. https://doi.org/10.48738/2022.iss1.105.

King, G., Bailey, G., 1985. The palaeoenvironment of some archaeological sites in Greece: the influence of accumulated uplift in a seismically active region. Proc.

Prehist. Soc. 51, 273–282. https://doi.org/10.1017/S0079497X0000712X.
Kopp, G.H., Roos, C., Butynski, T.M., Wildman, D.E., Alagaili, A.N., Groeneveld, L.F., Zinner, D., 2014. Out of Africa, but how and when? The case of hamadryas baboons (Papio hamadryas). J. Hum. Evol. 76, 154–164. https://doi.org/10.1016/j.jhevol.2014.08.003.
Kübler, S., Owenga, P., Reynolds, S.C., Rucina, S.M., King, G.C.P., 2015. Animal movements in the Kenya Rift and evidence for the earliest ambush hunting by hominins. Sci. Rep. 5, 14011. https://doi.org/10.1038/srep14011.
Lahr, M.M., Foley, R., 1994a. Multiple dispersals and modern human origins. Evol. Anthropol. 3, 48–60. https://doi.org/10.1002/evan.1360030206.
Lahr, M.M., Foley, R., 1994b. Multiple dispersals and modern human origins. Evol. Anthropol. 3, 48–60. https://doi.org/10.1002/evan.1360030206.
Lambeck, K., 1995. Late Pleistocene and Holocene sea-level change in Greece and south-western Turkey: a separation of eustatic, isostatic and tectonic contributions. Geophys. J. Int. 122, 1022–1044. https://doi.org/10.1111/j.1365-246X.1995.tb06853.x.
Lambeck, K., 1996. Sea-level change and shore-line evolution in Aegean Greece since Upper Palaeolithic time. Antiquity 70, 588–611. https://doi.org/10.1017/S0003598X00083733.
Lambeck, K., 2004. Sea-level change through the last glacial cycle: geophysical, glaciological and palaeogeographic consequences. Compt. Rendus Geosci. 336, 677–689. https://doi.org/10.1016/j.crte.2003.12.017.
Lambeck, K., Antonioli, F., Purcell, A., Silenzi, S., 2004. Sea-level change along the Italian coast for the past 10,000yr. Quat. Sci. Rev. 23, 1567–1598. https://doi.org/10.1016/j.quascirev.2004.02.009.
Lambeck, K., Purcell, A., Flemming, N.C., Vita-Finzi, C., Alsharekh, A.M., Bailey, G.N., 2011. Sea level and shoreline reconstructions for the Red Sea: isostatic and tectonic considerations and implications for hominin migration out of Africa. Quat. Sci. Rev. 30, 3542–3574. https://doi.org/10.1016/j.quascirev.2011.08.008.
Lambeck, K., Purcell, A., Johnston, P., Nakada, M., Yokoyama, Y., 2003. Water-load definition in the glacio-hydro-isostatic sea-level equation. Quat. Sci. Rev. 22, 309–318. https://doi.org/10.1016/S0277-3791(02)00142-7.
Lambeck, K., Purcell, A., Zhao, S., 2017. The North American Late Wisconsin ice sheet and mantle viscosity from glacial rebound analyses. Quat. Sci. Rev. 158, 172–210. https://doi.org/10.1016/j.quascirev.2016.11.033.
Lambeck, K., Rouby, H., Purcell, A., Sun, Y., Sambridge, M., 2014. sea level and global ice volumes from the last glacial maximum to the Holocene. Proc. Natl. Acad. Sci. U.S.A. 111, 15296–15303. https://doi.org/10.1073/pnas.1411762111.
Larrasoaña, J.C., Roberts, A.P., Rohling, E.J., 2013. Dynamics of green Sahara periods and their role in hominin evolution. PLoS One 8, e76514. https://doi.org/10.1371/journal.pone.0076514.
Leppard, T.P., 2014a. Modeling the impacts of Mediterranean island colonization by archaic hominins: the likelihood of an insular Lower Palaeolithic. J. Mediterr. Archaeol. 27, 231–254.
Leppard, T.P., 2014b. Response: the elusive insular Lower Palaeolithic and the problem of intentionality. J. Mediterr. Archaeol. 27, 275–278.
Leppard, T.P., Runnels, C., 2017. Maritime hominin dispersals in the Pleistocene: advancing the debate. Antiquity 91, 510–519. https://doi.org/10.15184/aqy.2017.16.
López, S., van Dorp, L., Hellenthal, G., 2015. Human dispersal out of Africa: a lasting debate. Evolutionary bioinformatics online 11, 57–68. https://doi.org/10.4137/EBO.S33489.
Lykousis, V., 2009. Sea-level changes and shelf break prograding sequences during the last 400ka in the Aegean margins: subsidence rates and palaeogeographic implications. Continent. Shelf Res. 29, 2037–2044. https://doi.org/10.1016/j.csr.2008.11.005.
Macaulay, V., Hill, C., Achilli, A., Rengo, C., Clarke, D., Meehan, W., Blackburn, J., Semino, O., Scozzari, R., Cruciani, F., Taha, A., Shaari, N.K., Raja, J.M., Ismail, P., Zainuddin, Z., Goodwin, W., Bulbeck, D., Bandelt, H.J., Oppenheimer, S., Torroni, A., Richards, M., 2005. Single, rapid coastal settlement of Asia revealed by analysis of complete mitochondrial genomes. Science 308, 1034–1036. https://doi.org/10.1126/science.1109792.
Madah, F., Mayerle, R., Bruss, G., Bento, J., 2015. Characteristics of tides in the red sea region, a numerical model study. Open J. Mar. Sci. 5, 193–209. https://doi.org/10.4236/ojms.2015.52016.
Martin-Short, R., Hill, J., Kramer, S.C., Avdis, A., Allison, P.A., Piggott, M.D., 2015. Tidal resource extraction in the Pentland Firth, UK: potential impacts on flow regime and sediment transport in the Inner Sound of Stroma. Renew. Energy 76, 596–607. https://doi.org/10.1016/j.renene.2014.11.079.
Martínez-Navarro, B., 2010. Early Pleistocene faunas of Eurasia and hominin dispersals. In: Fleagle, J.G., Shea, J.J., Grine, F.E., Baden, A.L., Leakey, R.E. (Eds.), Out of Africa I: the First Hominin Colonization of Eurasia. Springer Netherlands, Dordrecht, pp. 207–224. https://doi.org/10.1007/978-90-481-9036-2_13.
Mellars, P., 2006. Going east: new genetic and archaeological perspectives on the modern human colonization of Eurasia. Science 313, 796–800. https://doi.org/10.1126/science.1128402.
Mellars, P., Gori, K.C., Carr, M., Soares, P.A., Richards, M.B., 2013. Genetic and archaeological perspectives on the initial modern human colonization of southern Asia. Proc. Natl. Acad. Sci. U.S.A. 110, 10699–10704. https://doi.org/10.1073/pnas.1306043110.
Mitchell, A.J., Uličný, D., Hampson, G.J., Allison, P.A., Gorman, G.J., Piggott, M.D., Wells, M.R., Pain, C.C., 2010. Modelling tidal current-induced bed shear stress and palaeocirculation in an epicontinental seaway: the Bohemian Cretaceous Basin, Central Europe. Sedimentology 57, 359–388. https://doi.org/10.1111/j.1365-3091.2009.01082.x.
Mitchell, N.C., Sofianos, S.S., 2019. Origin of submarine channel north of hanish sill, red sea. In: Rasul, N.M.A., Stewart, I.C.F. (Eds.), Geological Setting, Palaeoenvironment and Archaeology of the Red Sea. Springer International Publishing, Cham, pp. 259–273. https://doi.org/10.1007/978-3-319-99408-6_12.
Mitrovica, J.X., Milne, G.A., 2003. On post-glacial sea level: I. General theory. Geophys. J. Int. 154, 253–267. https://doi.org/10.1046/j.1365-246X.2003.01942.x.
Murray, S.P., Johns, W., 1997. Direct observations of seasonal exchange through the Bab el Mandab Strait. Geophys. Res. Lett. 24, 2557–2560. https://doi.org/10.1029/97gl02741.
Nakada, M., Lambeck, K., 1987. Glacial rebound and relative sea-level variations: a new appraisal. Geophys. J. Int. 90, 171–224. https://doi.org/10.1111/j.1365-246X.1987.tb00680.x.
Oppenheimer, S., 2012. Out-of-Africa, the peopling of continents and islands: tracing uniparental gene trees across the map. Philos. Trans. R. Soc. Lond. Ser. B Biol. Sci. 367, 770–784. https://doi.org/10.1098/rstb.2011.0306.
Parkinson, S.D., Hill, J., Piggott, M.D., Allison, P.A., 2014. Direct numerical simulations of particle-laden density currents with adaptive, discontinuous finite elements. Geosci. Model Dev. (GMD) 7, 1945–1960. https://doi.org/10.5194/gmd-7-1945-2014.
Peltier, W.R., 1998. Postglacial variations in the level of the sea: implications for climate dynamics and solid-Earth geophysics. Rev. Geophys. 36, 603–689. https://doi.org/10.1029/98rg02638.
Petraglia, M.D., Alsharekh, A., 2003. The Middle Palaeolithic of Arabia: implications for modern human origins, behaviour and dispersals. Antiquity 77, 671–684. https://doi.org/10.1017/S0003598X00061639.
Petraglia, M.D., Breeze, P.S., Groucutt, H.S., 2019. Blue Arabia, green Arabia: examining human colonisation and dispersal models. In: Rasul, N.M.A., Stewart, I.C.F. (Eds.), Geological Setting, Palaeoenvironment and Archaeology of the Red Sea. Springer International Publishing, Cham, pp. 675–683. https://doi.org/10.1007/978-3-319-99408-6_30.
Phoca-Cosmetatou, N., Rabett, R.J., 2014. Discussion and debate: reflections on Pleistocene island occupation. J. Mediterr. Archaeol. 27, 255–259.
Piggott, M.D., Gorman, G.J., Pain, C.C., Allison, P.A., Candy, A.S., Martin, B.T., Wells, M.R., 2008. A new computational framework for multi-scale ocean modelling based on adapting unstructured meshes. Int. J. Numer. Methods Fluid. 56, 1003–1015. https://doi.org/10.1002/fld.1663.
Plaziat, J.C., Baltzer, F., Choukri, A., Conchon, O., Freytet, P., Orszag-Sperber, F., Raguideau, A., Reyss, J.L., 1998. Quaternary marine and continental sedimentation in the northern Red Sea and Gulf of Suez (Egyptian coast): influences of rift tectonics, climatic changes and sea-level fluctuations. In: Purser, B.H., Bosence, D.W.J. (Eds.), Sedimentation and Tectonics in Rift Basins Red Sea:- Gulf of Aden. Springer Netherlands, Dordrecht, pp. 537–573. https://doi.org/10.1007/978-94-011-4930-3_29.
QGIS Development Team, 2016. QGIS geographic information system. URL: https://qgis.org.
Rasul, N.M.A., Stewart, I.C.F., Vine, P., Nawab, Z.A., 2019. Introduction to oceanographic and biological aspects of the red sea. In: Rasul, N.M.A., Stewart, I.C.F. (Eds.), Oceanographic and Biological Aspects of the Red Sea. Springer International Publishing, Cham, pp. 1–9. https://doi.org/10.1007/978-3-319-99417-8_1.
Rohling, E.J., Grant, K.M., Roberts, A.P., Larrasoaña, J.C., 2013. Paleoclimate variability in the mediterranean and red sea regions during the last 500,000 Years: implications for hominin migrations. Curr. Anthropol. 54, S183–S201. https://doi.org/10.1086/673882.
Runnels, C., 2014. Early palaeolithic on the Greek islands. J. Mediterr. Archaeol. 27, 211–230.
Sakellariou, D., Galanidou, N., 2017. Aegean Pleistocene landscapes above and below sea-level: palaeogeographic reconstruction and hominin dispersals. In: Bailey, G.N., Harff, J., Sakellariou, D. (Eds.), Under the Sea: Archaeology and Palaeolandscapes of the Continental Shelf. Springer International Publishing, Cham, pp. 335–359. https://doi.org/10.1007/978-3-319-53160-1_22.
Sakellariou, D., Lykousis, V., Geraga, M., Rousakis, G., Soukisian, T., 2017. Late Pleistocene Environmental Factors of the Aegean Region (Aegean Sea Including the Hellenic Arc) and the Identification of Potential Areas for Seabed Prehistoric Sites and Landscapes. In: Flemming, N.C., Harff, J., Moura, D., Burgess, A., Bailey, G.N. (Eds.), Submerged Landscapes of the European Continental Shelf. https://doi.org/10.1002/9781118927823.ch15.
Sakellariou, D., Rousakis, G., Panagiotopoulos, I., others, 2019. Geological Structure and Late Quaternary Geomorphological Evolution of the Farasan Islands Continental Shelf, South Red Sea, SW Saudi Arabia. And Archaeology of the.
Scourse, J., Uehara, K., Wainwright, A., 2009. Celtic Sea linear tidal sand ridges, the Irish Sea Ice Stream and the Fleuve Manche: palaeotidal modelling of a transitional passive margin depositional system. Mar. Geol. 259, 102–111. https://doi.org/10.1016/j.margeo.2008.12.010.
Sergiou, S., Geraga, M., Rohling, E.J., Rodríguez-Sanz, L., Hadjisolomou, E., Paraschos, F., Sakellariou, D., Bailey, G., 2022. Influences of sea level changes and the South Asian Monsoon on southern Red Sea oceanography over the last 30 ka. Quat. Res. 1–19. https://doi.org/10.1017/qua.2022.16.
Smith, R.C., Hill, J., Collins, G.S., Piggott, M.D., Kramer, S.C., Parkinson, S.D., Wilson, C., 2016. Comparing approaches for numerical modelling of tsunami generation by deformable submarine slides. Ocean Model. 100, 125–140. https://doi.org/10.1016/j.ocemod.2016.02.007.
Smithsonian Institution, 2013. Global Volcanism Program. https://volcano.si.edu/. (Accessed 12 January 2022). accessed.
Sofianos, S.S., Johns, W.E., Murray, S.P., 2002. Heat and freshwater budgets in the Red Sea from direct observations at Bab el Mandeb. Deep-sea research. Part II.

Topical studies in oceanography 49, 1323–1340. https://doi.org/10.1016/S0967-0645(01)00164-3.
Spratt, R.M., Lisiecki, L.E., 2016. A Late Pleistocene sea level stack. Clim. Past 12, 1079–1092. https://doi.org/10.5194/cp-12-1079-2016.
Straus, L.G., 2001. Africa and iberia in the Pleistocene. Quat. Int.: the journal of the International Union for Quaternary Research 75, 91–102. https://doi.org/10.1016/S1040-6182(00)00081-1.
Uehara, K., Scourse, J.D., Horsburgh, K.J., Lambeck, K., Purcell, A.P., 2006. Tidal evolution of the northwest European shelf seas from the Last Glacial Maximum to the present. J. Geophys. Res. 111, 235. https://doi.org/10.1029/2006JC003531.
Walter, R.C., Buffler, R.T., Bruggemann, J.H., Guillaume, M.M., Berhe, S.M., Negassi, B., Libsekal, Y., Cheng, H., Edwards, R.L., von Cosel, R., Néraudeau, D., Gagnon, M., 2000. Early human occupation of the Red Sea coast of Eritrea during the last interglacial. Nature 405, 65–69. https://doi.org/10.1038/35011048.
Wells, M.R., Allison, P.A., Piggott, M.D., Gorman, G.J., Hampson, G.J., Pain, C.C., Fang, F., 2007. Numerical modeling of tides in the late pennsylvanian mid-continent seaway of north America with implications for hydrography and sedimentation. J. Sediment. Res. 77, 843–865. https://doi.org/10.2110/jsr.2007.075.
Wells, M.R., Allison, P.A., Piggott, M.D., Hampson, G.J., Pain, C.C., Gorman, G.J., 2010. Tidal modeling of an ancient tide-dominated seaway, Part 1: model validation and application to global early cretaceous (aptian) tides. J. Sediment. Res. 80, 393–410. https://doi.org/10.2110/jsr.2010.044.
Werner, F., Lange, K., 1975. A bathymetric survey of the sill area between the Red Sea and the Gulf of Aden. Geologisches Jarbuch D 13, 125–130.
Wessel, P., Smith, W.H.F., 1996. A global self-consistent, hierarchical, high-resolution shoreline database. J. Geophys. Res. 101, 8741–8743.
Wilmes, S.B., Green, J.A.M., 2014. The evolution of tides and tidal dissipation over the past 21,000 years. J. Geophys. Res. C Oceans 119, 4083–4100. https://doi.org/10.1002/2013JC009605.
Winder, I.C., Devès, M.H., King, G.C.P., Bailey, G.N., Inglis, R.H., Meredith-Williams, M., 2015. Evolution and dispersal of the genus Homo: a landscape approach. J. Hum. Evol. 87, 48–65. https://doi.org/10.1016/j.jhevol.2015.07.002.